Multiple-scattering distributions and angular dependence of the energy loss of slow protons in copper and silver

E. D. Cantero, G. H. Lantschner, J. C. Eckardt, F. C. Lovey, and N. R. Arista
Centro Atómico Bariloche and Instituto Balseiro, Comisión Nacional de Energía Atómica, 8400 S. C. de Bariloche, Argentina
(Received 29 December 2009; published 14 April 2010)

Measurements of angular distributions and of the angular dependence of the energy loss of 4-, 6-, and 9-keV protons transmitted through thin Cu and Ag polycrystalline foils are presented. By means of standard multiple-scattering model calculations it is found that a $V(r) \propto r^{-2.8}$ potential leads to significantly better fits of the angular distributions than the standard Thomas Fermi, Lenz-Jensen, or Ziegler-Biersack-Littmark potentials. A theoretical model for the angular dependence of the energy loss based on considering geometric effects on a frictional inelastic energy loss plus an angular-dependent elastic contribution and the effects of foil roughness reproduces the experimental data. This agrees with previous results in Au and Al, therefore extending the applicability of the model to other metallic elements.

DOI: 10.1103/PhysRevA.81.042902 PACS number(s): 34.50.Bw, 34.20.Cf

I. INTRODUCTION

The physics of the interactions of atomic projectiles with thin solid films is a subject of current interest due to its relevance both in basic research and numerous applications, such as ion implantation, health physics, radiation damage, space flight, and fast semiconductor devices. Two basic quantities used to describe these interactions are the angular and energy distributions of an initially monoenergetic ion beam after traversing a target. In the low-energy regime (below 25 keV/amu) there are few published experimental data of these distributions. Some of the reasons of this scarcity are the technical difficulties involved in the construction of smooth self-supporting films with thicknesses below 30 nm, which are required for this type of experiment.

Several theoretical approaches regarding multiple-scattering were successfully applied to the study of fast ions interactions [1–3]. In Ref. [3], similarity properties were found in the multiple scattering distributions after applying the reduced variables formalism of Ref. [1]. A recent review of the different theories can be found in Ref. [4]. On the other hand, for low-energy ions no adequate tests of the multiple-scattering theories in solids have been made. Moreover, the well-known interatomic potentials of Thomas-Fermi and Lenz-Jensen, among others, which are frequently used as standard for high-energy ion interactions, are not adequate in this low-energy range [5,6]. Therefore, the search of different alternatives for the interaction potential is of interest.

Since the early 2000s several studies of the angular distributions and of the angular dependence of the energy loss of low-energy light ions have been published [7–10]. For polycrystalline samples, a simple model to evaluate the angular dependence of the energy loss of low-energy protons was proposed and successfully compared with experimental data of 9-keV protons transmitted through thin aluminium and gold films [7]. The measured angular distributions were well described by the multiple-scattering formalism of Ref. [3] considering power potentials $V(r) \propto r^{-n}$ and using $n = 2$ for Al and $n = 2.8$ for Au.

The objective of this work is to investigate experimentally and theoretically the angular distribution and the energy loss of very low energy protons after being transmitted through thin polycrystalline foils of Cu and Ag. By measurements with different elements we test the validity of the simple model for the angular dependence of the energy loss of Ref. [7] and a more extended applicability of the simple power potentials proposed in that reference.

In the following section the experimental procedure and the data analysis is presented. The main theoretical aspects of this work are shown in Sec. III. The results are discussed in Sec. IV and the conclusions are presented in Sec. V. An appendix is included with some explicit definitions regarding the potentials and scattering cross sections used in the presented calculations.

II. EXPERIMENTAL PROCEDURE AND DATA ANALYSIS

The energy loss and angular distribution determinations were made using the transmission technique, complemented by an electrostatic ion energy analysis. The proton beams were produced with a low-energy accelerator located at the Centro Atómico Bariloche, Argentina. The ions were generated in a hot-cathode ion source followed by acceleration and focusing stages, and using a Wien filter to separate different beam components. An electrostatic deflection of the beam eliminated the neutral beam component. The energy dispersion of the incident beams was a few eV's.

The targets were mounted perpendicularly to the incoming beam direction, followed by a rotatable 127° cylindrical electrostatic energy analyzer which allowed the energy analysis at different exit angles θ. The angular acceptance of the analyzer was 0.5° in one direction and 1.6° in the perpendicular one.

The polycrystalline self-supported foils of Cu and Ag were made by evaporation on a very smooth plastic substrate that was subsequently dissolved [11]. The thicknesses Δx were 157 ± 8 Å for the copper target and 250 ± 12 Å for the silver one. These values were obtained by comparison with previous stopping power determinations [12,13]. The stated uncertainties arise from our energy loss determinations and do not include possible errors of the reference stopping power values. The thickness inhomogeneities of the targets were characterized by upper bounds for the roughness coefficients, being $\rho_{Cu} < 14\%$ and $\rho_{Ag} < 12\%$. These bounds were obtained assuming that all the energy straggling of the spectra is

 ©2010 The American Physical Society

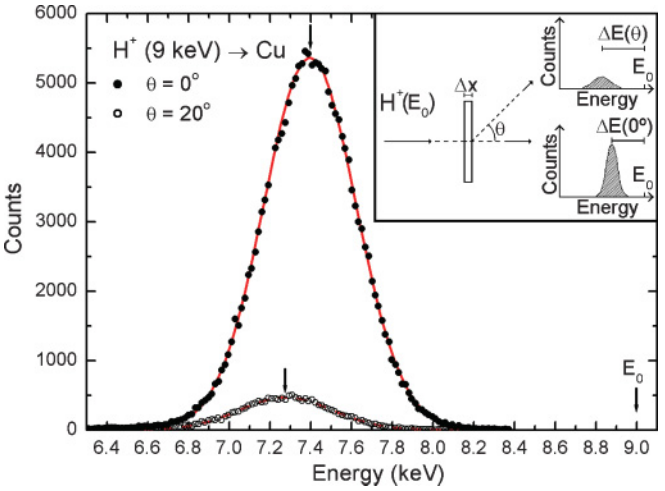

FIG. 1. (Color online) Energy spectra of 9-keV protons transmitted through the Cu target. Closed circles: ions emerging in the forward direction. Open circles: ions emerging at 20°. Solid lines show the Gaussian fits. Inset: basic scheme of the collision geometry.

due to these inhomogeneities. For both elements a transmission electron microscopy analysis revealed a polycrystalline structure with randomly oriented crystallites of sizes ∼5 to 20 nm. In the case of Cu, the diffraction ring pattern indicates the presence of a thin oxidation layer. This thin layer did not affect the present measurements beyond the experimental uncertainties.

The experimental procedure consisted of measuring the energy distributions at different exit angles maintaining a constant ion dose. The angular distributions were obtained by integrating the energy spectra corresponding to the different selected angles.

The energy loss was determined as the difference between the incident energy E_0 and the most probable exit energy E_1.

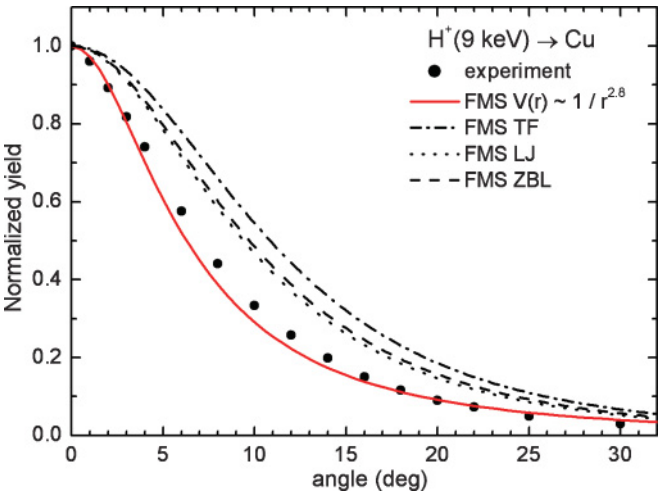

FIG. 2. (Color online) Normalized angular distributions of 9-keV protons transmitted through Cu. The solid line shows the multiple-scattering distributions calculated for a $V(r) \sim r^{-2.8}$ potential. The dotted, dashed, and dot-dashed lines correspond to the multiple-scattering distributions considering Lenz-Jensen, Ziegler-Biersack-Littmark, and the Thomas-Fermi potentials, respectively.

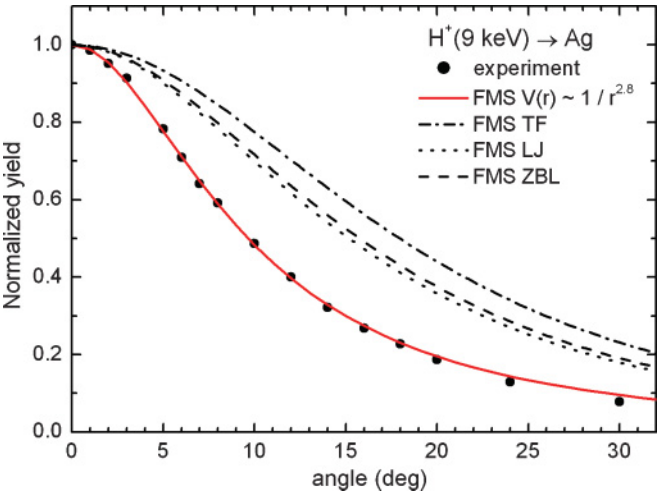

FIG. 3. (Color online) Normalized angular distributions of 9-keV protons transmitted through Ag. Lines: same as in Fig. 2.

As examples in Fig. 1 we plot two energy spectra of 9-keV protons traversing a Cu foil. One corresponds to the exit angle $\theta = 0°$ and the other to $\theta = 20°$. In the inset of the same figure a basic scheme of the collision geometry is shown.

III. THEORETICAL MODELS AND CONSIDERATIONS

A. Angular distributions

In this work we compare the experimental results of the angular distributions with the theoretical formalism of Sigmund and Winterbon [3]. The multiple-scattering (MS) formulation is based on the Bothe equation [14], which can be derived by a collision summation method or by a transport equation. This formalism assumes that the scattering centers in the target are randomly distributed in space, that each collision event can be described under the binary collision approach, and that the scattering angles are small on an absolute scale. The

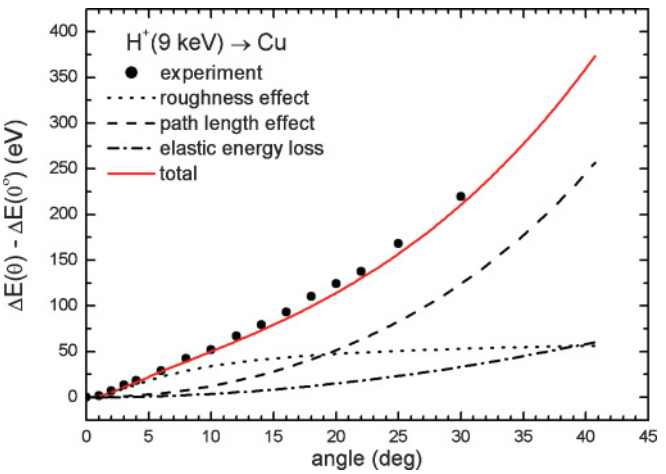

FIG. 4. (Color online) Angular dependence of the energy loss of 9-keV protons transmitted through a Cu foil (referred to the energy loss in the forward direction). Dashed line: increase of the energy loss due to path-length enlargement. Dash-dotted line: contribution of elastic scattering. Dotted line: effect of the foil roughness. Solid line: sum of the three contributions.

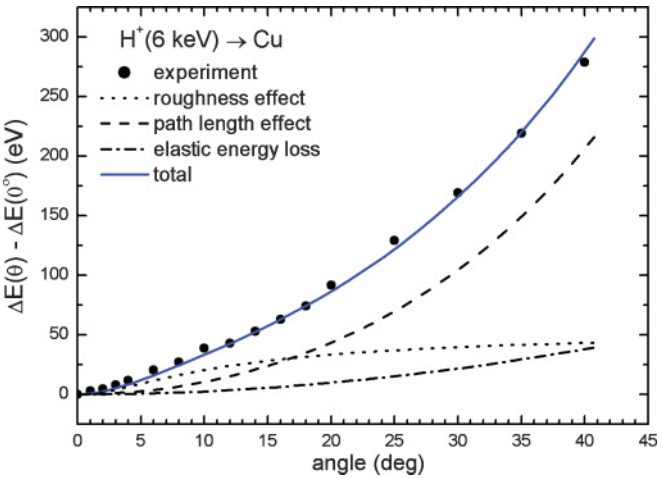

FIG. 5. (Color online) Angular dependence of the energy loss of 6-keV protons transmitted through a Cu foil (referred to the energy loss in the forward direction). Lines: same as in Fig. 4.

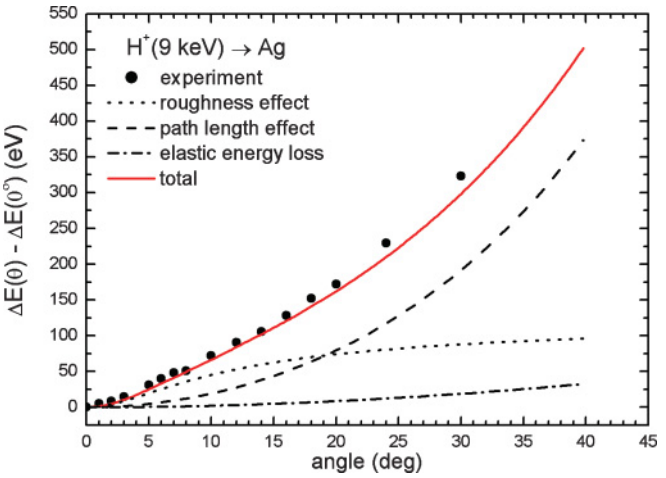

FIG. 7. (Color online) Angular dependence of the energy loss of 9-keV protons transmitted through a Ag foil (referred to the energy loss in the forward direction). Lines: same as in Fig. 4.

effects produced by the energy loss of the projectiles during their paths inside the target were considered by using the mean energy of the ions for the calculations of the MS distributions, following Ref. [15].

The MS distributions corresponding to four different scattering potentials were calculated:

(a) Power potential $V(r) \propto r^{-n}$, (b) Thomas-Fermi potential (TF), (c) Lenz-Jensen potential (LJ), and (d) Ziegler-Biersack-Littmark potential (ZBL).

For the power potential, the proportionality constant depends on n, and its value was fixed in this work following Ref. [16], although many authors use it as a free parameter. More details on the potentials and their corresponding scattering functions are given in the appendix.

The TF, LJ, and ZBL potentials, widely used for swift heavy ions, are based on theoretical (TF, LJ) or statistical (ZBL) approximations whose validity for slow light projectiles is uncertain. In this work, however, we included the MS calculations using these potentials in order to show the magnitude of the deviations that may appear when they are used to describe low-energy projectiles scattering.

As an alternative, we consider here the so-called power potential $V(r) \propto r^{-n}$, showing that it provides a convenient *effective* potential to represent the angular distributions on the low-energy range for the cases studied in this work. We note that the comparison between experimental and calculated MS distributions should be understood as an approach that gives information about mean properties of the interatomic potentials in the range of impact parameters scanned by the projectiles rather than a precise description of the actual shape of these potentials.

B. Angular dependence of the energy loss

The model used to calculate the angular dependence of the energy loss is the one proposed in Ref. [7]. It considers three different contributions to the variation of the energy loss ΔE with the observation angle θ:

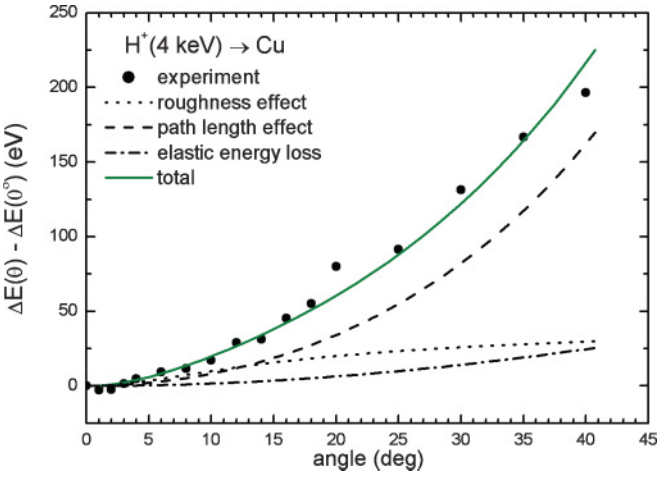

FIG. 6. (Color online) Angular dependence of the energy loss of 4-keV protons transmitted through a Cu foil (referred to the energy loss in the forward direction). Lines: same as in Fig. 4.

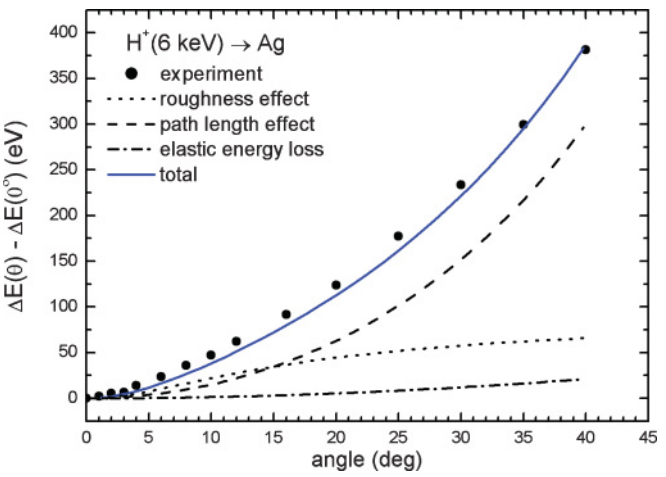

FIG. 8. (Color online) Angular dependence of the energy loss of 6-keV protons transmitted through a Ag foil (referred to the energy loss in the forward direction). Lines: same as in Fig. 4.

(i) changes in the energy loss due to path length increase, (ii) the variation of the elastic energy loss, and (iii) the effect of the foil roughness.

This theoretical approach considers that the angular deflection is mainly due to a single collision with an angle $\theta_{SC} \simeq \theta$ near the observation angle, preceded and followed by small angle collisions. This feature was studied using an analytical formalism based on multiple-scattering functions as well as with Monte Carlo simulations in Ref. [17]. Under these assumptions, the first two contributions are calculated for light projectiles ($M_1 \ll M_2$) as

$$\Delta E_{\mathrm{elec}}(\theta) - \Delta E_{\mathrm{elec}}(0) = \frac{1}{2}\left(\frac{1}{\cos(\theta)} - 1\right)\Delta E_{\mathrm{elec}}(0), \quad (1)$$

and

$$\Delta E_{\mathrm{nucl}}(\theta) - \Delta E_{\mathrm{nucl}}(0) \simeq \Delta E_{\mathrm{nucl}}(\theta) \simeq 4\frac{M_1 M_2}{(M_1 + M_2)^2} E \sin^2(\theta/2). \quad (2)$$

The inhomogeneities in foil thickness also lead to an angular dependence of the energy loss. This is produced because projectiles traversing thicker sections of the target are more likely deflected to larger angles and lose more energy than those detected at small angles.

For projectiles with mean energy loss $\overline{\Delta E}$ transmitted through a foil of thickness Δx and roughness coefficient ρ, this contribution is given by [18]

$$\Delta E(\theta)_{\mathrm{rough}} - \Delta E(0)_{\mathrm{rough}} = \rho^2\,\overline{\Delta E}\left(\frac{\partial \ln |F_{\mathrm{MS}}(\theta, \Delta x)|}{\partial \ln \Delta x} - \frac{\partial \ln |F_{\mathrm{MS}}(0, \Delta x)|}{\partial \ln \Delta x}\right), \quad (3)$$

where $F_{\mathrm{MS}}(\theta, \Delta x)$ is the multiple-scattering distribution of the ions.

The total variation of the energy loss with the observation angle was calculated as the sum of these three contributions.

IV. RESULTS AND DISCUSSION

A. Angular distributions

The normalized angular distributions for 9-keV protons in Cu and Ag are plotted in Figs. 2 and 3. The curves obtained using the standard Lenz-Jensen, Thomas-Fermi, and Ziegler-Biersack-Littmark scattering potentials lead to angular distributions significantly wider than the experimental ones. The distributions calculated using the power potential with $n = 2.8$ agree well with the experimental data. The same result was previously observed for the angular distributions of low-energy protons transmitted through Au films [7], where the MS distributions were also well described by using a power potential with $n = 2.8$.

The fact that the MS distributions of low-energy protons in Cu, Ag, and Au can be well described by a power potential with the same exponent indicates the existence of a similarity in the scattering potentials of low-energy ions for these three metals. Note that the power potential $V(r) \propto r^{-2}$ which adjusts angular distributions of protons in Al differs significantly.

The relatively high values of n obtained here are in agreement with Lindhard's criterion (cf. Ref. [1], p. 15) for the behavior of the interatomic potentials in the low-energy range, for weakly penetrating trajectories ($r \gtrsim a$, where a is the screening radius [1]). In this range of distances the role of the outermost electronic shells may be significant, and so one may expect a similar behavior of the transition metals Cu, Ag, and Au. This may be the reason for the same exponent of the power potential obtained for these cases. We think this shows a subject of much interest for a more detailed theoretical study of interaction potentials in the low-energy range.

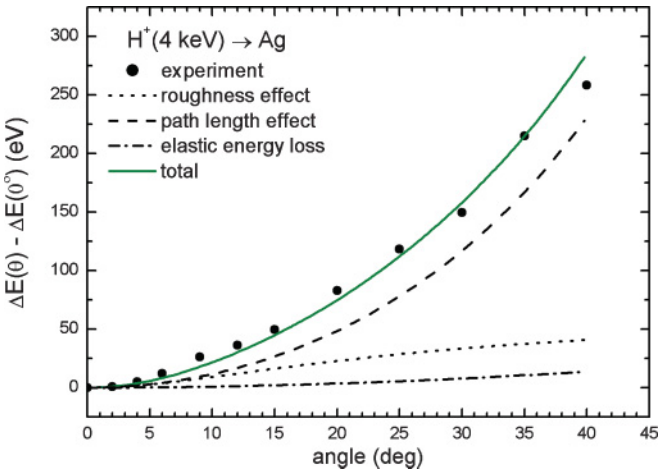

FIG. 9. (Color online) Angular dependence of the energy loss of 4-keV protons transmitted through a Ag foil (referred to the energy loss in the forward direction). Lines: same as in Fig. 4.

B. Angular dependence of the energy loss

In Figs. 4 to 6 we show the angular dependence of the mean energy loss of protons of 9, 6, and 4 keV after traversing a 157 Å Cu film. The results of the model calculation with its different contributions are also shown. The foil roughness contribution was calculated using the MS function corresponding to the power potential $V(r) \propto r^{-2.8}$ and a roughness coefficient $\rho_{\mathrm{Cu}} = 10\%$. This value leads to the best agreement with the experimental data and lies below the previously mentioned roughness bound.

In Figs. 7 to 9 we show the experimental data and calculations corresponding to protons in a 250 Å Ag foil. The foil roughness contribution was evaluated using also the MS function calculated with the $n = 2.8$ power potential. The roughness coefficient used here was $\rho_{\mathrm{Ag}} = 11\%$.

We observe a very good agreement between the experimental data and the model for the angular dependence of the energy loss of protons. These results show the applicability of this theoretical approach for protons in polycrystalline Cu and Ag targets at several projectile energies for exit angles up to 40°. We note that this model includes in a realistic way the main mechanisms of the angular dependence of the energy loss.

V. CONCLUDING REMARKS

The present angular distribution and energy-loss measurements for H^+ in Cu and Ag in the low-energy range from 4 to 9 keV and related model calculations together with previous results for Au and Al [7] lead to the following conclusions.

Applying a multiple-scattering formalism [3] we find that the widespread Lenz-Jensen, Thomas-Fermi, and Ziegler-Biersack-Littmark potentials lead to significantly broader angular distributions than the experiments for Cu, Ag, and Au.

These experimental distributions for Cu, Ag, and Au can be theoretically described using the same power potential $V(r) \propto r^{-2.8}$ for the three elements. This reflects the similarity of the screening contribution by the outer electrons of these metals. Note that in the case of Al the most adequate power potential is r^{-2}.

The angular dependence of the energy loss for protons of energies between 4 to 9 keV in Cu and Ag is very well described by the model of Ref. [7] which considers the effects of path-length enlargement, elastic energy loss, and foil roughness. These results permit to extend the validity of the model to a wider range of materials.

ACKNOWLEDGMENTS

This work was partially supported by ANPCYT of Argentina (Project PICT 903/07). E.D.C. acknowledges support from the Consejo Nacional de Investigaciones Científicas y Técnicas (CONICET), Argentina.

APPENDIX: SCREENING POTENTIALS AND SCATTERING CROSS SECTION

In the multiple-scattering calculations we used the formalism of the scaled angular distributions of Ref. [3], where the influence of the interaction potential on the differential scattering cross section is described by means of the well-known $f(t^{1/2})$ scattering function.

For the TF and the LJ potentials we used the results of Ref. [3]

$$f(t^{1/2}) = f(\tilde{\phi}) = \Lambda \tilde{\phi}^{1-2m}[1 + (2\Lambda\tilde{\phi}^{2-2m})^q]^{-1/q}, \quad \text{(A1)}$$

where $m = 0.311$, $\Lambda = 1.70$, and $q = 0.588$ for the Thomas-Fermi screening and $m = 0.191$, $\Lambda = 2.92$, and $q = 0.512$ for the Lenz-Jensen screening.

In the case of power potentials

$$V(r) = \frac{Z_1 Z_2}{r} \frac{k_n}{n} \left(\frac{a}{r}\right)^{n-1}, \quad \text{(A2)}$$

the scattering function is analytically given by [1]

$$f(\tilde{\phi}) = \lambda_n \tilde{\phi}^{1-2/n}. \quad \text{(A3)}$$

Here λ_n is a numerical constant evaluated following [1,16]

$$\lambda_n = \left(\frac{2}{n}\right)\left(\frac{k_n \gamma_n}{2}\right)^{2/n}, \quad \text{(A4)}$$

with $\gamma_n = \frac{1}{2}B(\frac{1}{2}, \frac{n+1}{2})$ and $k_n = n\,(\frac{n-1}{0.8853\ e})^{n-1}$.

We made use of the approximation formulas of Ref. [19] for the scattering function of the potential of Ziegler, Biersack, and Littmark [20]

$$f(\tilde{\phi}) = \begin{cases} f_1(\tilde{\phi}) & \text{for } \tilde{\phi} \leqslant \tilde{\phi}^* \\ f_2(\tilde{\phi}) & \text{for } \tilde{\phi} > \tilde{\phi}^* \end{cases}$$

with

$$f_1(\tilde{\phi}) = \tilde{\phi}[a_1 \ln \tilde{\phi} + a_2(\ln \tilde{\phi})^2 + a_3(\ln \tilde{\phi})^3 + c_1 + c_2\tilde{\phi}]$$

$$f_2(\tilde{\phi}) = \frac{b_1 + \tilde{\phi}/2}{b_2 + b_3\tilde{\phi} + \tilde{\phi}^2}, \quad \text{(A5)}$$

where the parameters are

$$\begin{aligned} a_1 &= -0.228, \quad a_2 = 0.243, \quad a_3 = -0.117 \\ b_1 &= 1.50, \quad b_2 = 3.05, \quad b_3 = 3.17 \\ \tilde{\phi}^* &= 0.380, \quad c_1 = 0.671, \quad c_2 = 0.522. \end{aligned} \quad \text{(A6)}$$

[1] J. Lindhard, V. Nielsen, and M. Scharff, K. Dan. Vidensk. Selsk. Mat. Fys. Medd. **36**, 10 (1968).
[2] L. Meyer, Phys. Status Solidi **44**, 253 (1971).
[3] P. Sigmund and K. B. Winterbon, Nucl. Instrum. Methods **119**, 541 (1974).
[4] G. Amsel, G. Battistig, and A. L'Hoir, Nucl. Instrum. Methods B **201**, 325 (2003)
[5] G. V. Dedkov, Phys. Status Solidi A **149**, 453 (1995).
[6] H. Winter and A. Shüller, Nucl. Instrum. Methods B **232**, 165 (2005)
[7] M. Famá, G. H. Lantschner, J. C. Eckardt, C. D. Denton, and N. R. Arista, Nucl. Instrum. Methods B **164**, 241 (2000).
[8] M. Famá, G. H. Lantschner, J. C. Eckardt, N. R. Arista, J. E. Gayone, E. Sanchez, and F. Lovey, Nucl. Instrum. Methods B **193**, 91 (2002).
[9] C. D. Archubi, C. Denton, J. C. Eckardt, G. H. Lantschner, F. Lovey, J. Valdés, C. Parra, F. Zappa, and N. R. Arista, Phys. Status Solidi B **241**, 2389 (2004).
[10] E. A. Figueroa, E. D. Cantero, J. C. Eckardt, G. H. Lantschner, M. L. Martiarena, and N. R. Arista, Phys. Rev. A **78**, 032901 (2008).
[11] A. Valenzuela and J. C. Eckardt, Rev. Sci. Instrum. **42**, 127 (1971).
[12] J. E. Valdés, J. C. Eckardt, G. H. Lantschner, and N. R. Arista, Phys. Rev. A **49**, 1083 (1994).
[13] J. E. Valdés, G. Martinez Tamayo, G. H. Lantschner, J. C. Eckardt, and N. R. Arista, Nucl. Instrum. Methods B **73**, 313 (1993).
[14] W. Bothe, Z. Phys. **5**, 63 (1921).
[15] J. E. Valdés and N. R. Arista, Phys. Rev. A **49**, 2690 (1994).
[16] N. Bohr, K. Dan. Vidensk. Selsk. Mat. Fys. Medd. **18**, 8 (1948).
[17] M. Famá, G. H. Lantschner, J. C. Eckardt, and N. R. Arista, Nucl. Instrum. Methods B **174**, 16 (2001).
[18] M. M. Jakas and N. E. Capuj, Nucl. Instrum. Methods B **36**, 491 (1989).
[19] H. J. Kang, E. Kawatoh, and R. Shimizu, Jpn. J. Appl. Phys. **23**, L262 (1984).
[20] J. F. Ziegler, J. Biersack, and U. Littmark, *The Stopping and Range of Ions in Matter* (Pergamon Press, Oxford, 1985).